

Pyrolysis of Thick Biomass Particles: Experimental and Kinetic Modelling

Guillaume Gauthier^a, Thierry Melkior^a, Sylvain Salvador^b, Michele Corbetta^c, Alessio Frassoldati^c, Sauro Pierucci^c, Eliseo Ranzi^c, Hayat Bennadji^d, Elizabeth M. Fisher^d

^aCEA – LITEN – Laboratory of Biomass Technologies, 17 rue des Martyrs, 38054 Grenoble Cedex 09, France

^bCentre RAPSODEE, UMR 5302 CNRS, Mines-Albi, Route de Teillet, 81013 Albi CT Cedex 09, Albi, France

^cDipartimento di Chimica, Materiali e Ingegneria Chimica “Giulio Natta”, Politecnico di Milano, Piazza Leonardo da Vinci 32, 20131 Milano, Italy

^dSibley School of Mechanical and Aerospace Engineering, Upson Hall, Cornell University, Ithaca, NY 14853, USA
guillaume.gauthier@cea.fr

The aim of this work is to analyze some new experimental data of pyrolysis of thick woody biomass particles with the help of a general and comprehensive mathematical model. This multiphase and multiscale problem involves strong interactions between chemical kinetics, both in the solid and in the gas phase, and heat/mass transfer phenomena.

Detailed experimental measurements have been obtained in an original lab scale reactor. This setup is designed to measure the products yielded along the pyrolysis of a single biomass (beech) particle as well as the temperature profiles into the sample. Experiments are carried out with pyrolysis temperatures ranging between 723 K and 1073 K. Lower-temperature pyrolysis data for poplar from a second reactor are also presented.

These results constitute a very useful data set to tune and validate a predictive multistep kinetic model of biomass pyrolysis (Ranzi et al. 2008) and to analyse and discuss the relative effect of different phenomena. The thermal behavior of the pyrolysis process is particularly highlighted.

1. Introduction

Environmental protection and fossil fuel depletion are some of the driving forces which push technological research towards the development of alternative fuels. Second generation biomass-to-biofuels is an interesting route, able to transform an abundant and well distributed feedstock into fuels with properties similar to conventional fossil fuels (Mendes and Figueiredo 2011). Moreover the lignocellulosic biomass is low in sulfur, resulting in a more ecological fuel (Catoire et al. 2008). Thermo-chemical conversion is one of the main approaches used to produce bio-oils, derived from the de-polymerization and fragmentation reactions of the three key biomass building blocks: cellulose, hemicelluloses and lignin. The selectivity of the process towards gas and liquid products is strongly affected by the thermal treatment used. In addition, for greater economic viability, it is suggested to use thick biomass particles as the feedstock, reducing grinding costs. This nevertheless increases the modeling complexity, due to mass and heat transfer limitations (Park et al. 2010).

Thermal gradients into the sample during pyrolysis are of negligible importance when studying the combustion or gasification of a thin particle. In the thermally thin regime, the characterization of biomass, the description of the release of the species, and their chemical evolution in the gas phase were studied and verified relating to thermal degradation of different biomass in a previous paper (Ranzi et al. 2008). The current work carefully analyses the thermal features of the pyrolysis of thick biomass particles.

Recent literature reports interesting pyrolysis experiments which show some unusual thermal behaviors (Park et al. 2010) and (Bennadji et al. 2013). Temperature profiles within the core of biomass particles, subjected to pyrolysis, exhibit a thermal sink, followed by a sharp peak, which overtakes the surface

thermal profile. The experimental fact could be explained on the basis of the process kinetics, which is described by both endothermic and exothermic reactions. A first endothermic stage corresponds to a primary release of volatile species, and a second exothermic period mainly corresponds to the successive transformations of the solid residue to final char.

New experiments are presented, and the previous (Ranzi et al. 2008) multistep kinetic model of biomass pyrolysis is further extended and validated in this work. The influence of exothermic and endothermic phenomena on temperature profiles inside the sample is discussed.

2. Experimental

2.1 Samples

Each experiment is carried out with a single beech wood particle, which is a cylinder, 20mm in diameter and 30mm in height. Sample dimensions are representative of typical centimetre-scale woodchip (NF EN 14961-1). The grain direction is parallel to the cylinder axis. All samples originate from the same trunk in order to limit the dispersion of the results due to feedstock variability. Samples are first dried in an oven at 378 K during 12h following the procedure NF EN 14774, and subsequently stored in a desiccator.

The wood elemental composition is found to be 48.70% in carbon, 6.04% in hydrogen and 44.46% in oxygen. Oxygen content is obtained by subtraction knowing that ash content is 0.80% at 823°C. The proximate analysis results from FCBA Grenoble Laboratory are: cellulose 41% \pm 1%, hemicelluloses 30% \pm 2% and lignin 25% \pm 2%.

2.2 Experimental device

The experimental device is depicted in Figure 1.

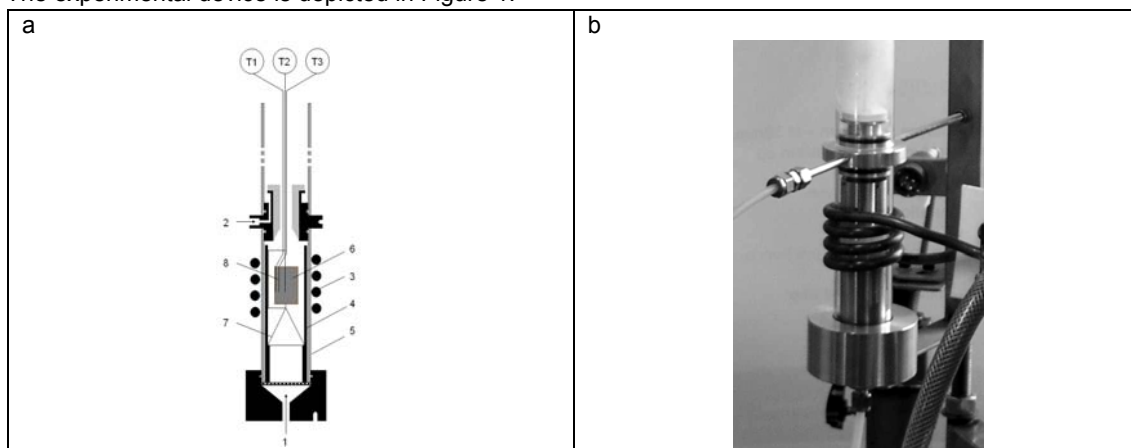


Figure 1: a: Experimental device 1: Nitrogen inlet ($2 \text{ NL}\cdot\text{min}^{-1}$) ; 2: Nitrogen inlet (from 1 to 3 $\text{NL}\cdot\text{min}^{-1}$) ; 3: Inductor ; 4: Inconel pipe heated by induction ; 5: Quartz pipe ; 6: Wood sample ; 7: sample holder ; 8: thermocouples. b: Photograph of the experimental device.

This equipment has been developed to study the pyrolysis of a single centimetre-scale sample. A 12kW induction furnace heats an Inconel pipe with a four-coil inductor. The temperature of the Inconel pipe can not exceed 1573 K. The temperature at the surface of the Inconel pipe is measured and controlled with a two-color pyrometer (IMPAC infratherm). The power of the inductor is controlled, with a GEFTRAN 2500 regulator, to maintain the temperature of the Inconel pipe at the chosen value.

With this equipment, the heating rate of the Inconel pipe can reach $773 \text{ K}\cdot\text{s}^{-1}$. Pyrolysis temperatures lie between 723 K and 1073 K.

The Inconel pipe is swept by nitrogen ($2 \text{ NL}\cdot\text{min}^{-1}$) to carry away the vapors produced during pyrolysis. Above the Inconel pipe, this flow is mixed with nitrogen at ambient temperature ($1 \text{ to } 3 \text{ NL}\cdot\text{min}^{-1}$) to cool down the volatile matter and condense a first fraction of organic vapors. Thermocouples (K type, 0.5-mm-ID) are imbedded in wood sample to record the internal temperature at different radii (on the centre and at 5 mm and 8 mm from the particle axis), all at an axial position 2 cm below the top of the particle.

A second set of experiments were performed with cylindrical poplar samples of similar dimensions ($D=1.9$ and 2.54 cm ; $L=4 \text{ cm}$) in a heated turbulent nitrogen flow. The 1.9-cm data was presented, and the apparatus was described, by (Bennadji et al. 2013). These experiments used gas temperatures below 700 K, conditions with relevance to biochar production conditions for soil amendment. Sheathed 0.25-mm thermocouples were situated on the centreline, at an axial position of 1 cm from the end of the particle.

3. Biomass characterization, physical and multistep kinetic models of biomass pyrolysis

The modeling approach is described and an extended version of (Ranzi et al. 2008) multistep kinetic model is presented.

3.1 Biomass characterization

Biomass is characterized in terms of the three major components: cellulose, hemicelluloses, and lignin, together with inert ashes and moisture. Lignin is approximated by a mixture of reference components due to its complex chemical structure. They are identified by LIG-C, LIG-H and LIG-O which reflect their characteristic of being richer in carbon, hydrogen and oxygen respectively.

In previous work (Ranzi et al. 2008), we proposed a method to characterize the biomass feedstock on the basis of its elemental composition and its general cellulose/hemicelluloses/lignin composition. Table 1 shows the results of this procedure applied to the biomass described in the experimental part.

Table 1: Biomass characterization in terms of reference components

Reference component	Atomic composition	Weight fraction (daf basis)
Cellulose	$C_6H_{10}O_5$	0.420
Hemicelluloses	$C_5H_8O_4$	0.315
LIGC	$C_{15}H_{14}O_4$	0.130
LIGH	$C_{22}H_{28}O_9$	0.016
LIGO	$C_{20}H_{22}O_{10}$	0.119

3.2 Thick particles and balance equation at the particle scale, physical model

At the particle scale, thermally thick particles exhibit significant internal temperature and mass gradients. The Biot number, defined as in equation (1), is a useful ratio to evaluate the extent of the temperature gradients. Large external heating rates and low thermal conductivity of thick particles create a Biot number >1 and temperature gradients inside the particle:

$$Bi = \frac{h \cdot d_p}{k} \quad (1)$$

where h is the external heat-transfer coefficient, k is the thermal conductivity, and d_p is the equivalent diameter of the solid particle.

The equivalent spherical diameter of the particles:

$$d_p = \frac{6 \cdot V_p}{S_p} \quad (2)$$

with V_p and S_p being the particle volume and surface, respectively.

Simulation results are obtained using in-house software. One-dimensional spherical coordinates are used to describe the gradients inside isotropic particles. Gradients of temperature, solid fuel composition, and gas concentrations both inside and outside the particle are predicted by the model, provided that the proper balance equations and boundary conditions are established.

3.3 Multistep kinetic model of biomass pyrolysis

The multistep kinetic model presented in this paper is a further extension of the previous one (Ranzi et al. 2008). The multistep kinetic model of biomass pyrolysis is based on conventional multistep devolatilization models of the three main biomass components - cellulose, hemicelluloses, and lignin - and gives detailed information on yields composition of gas, tar, and solid residue. Successive gas phase reactions of the released volatile species are then described by a general kinetic scheme of pyrolysis.

(Blondeau and Jeanmart 2012) have recently used the previous version and shown some discrepancies between simulated and experimental data. They studied the pyrolysis of cylindrical beech wood particles ranging from 100 μm to 2 mm in industrial boiler conditions. They suggested some modifications to the (Ranzi et al. 2008) pyrolysis mechanism in order to better predict the gas and tar species emissions, by a compared analysis of two pyrolysis mechanisms.

Table 2 gives the full details of a new version of the multistep kinetic model, including the heats of reaction. As far as the mechanism of cellulose is concerned, the heats of reaction agree well with the ones

estimated by (Milosavljevic et al. 1996). The char formation is an exothermic reaction releasing ~2000 kJ/kg of char formed, while the tar release is endothermic, absorbing ~500 kJ/kg of volatiles produced. The extended version is validated by comparison between simulated and experimental temperature profiles inside a biomass sample. Three experimental data sets are used for the validation: from the devices described in the experimental part and from (Park et al. 2010) studies. Results of comparison are presented on Figures 3, 4.a and 5.a. Simulated profiles agree satisfactorily with experimental ones.

Table 2: Multistep kinetic scheme of biomass pyrolysis.

Reaction	Kinetic constant* [s ⁻¹]	Heat of Reaction [kJ.kg ⁻¹]
CELL → CELLA	$8 \times 10^{13} \exp(-45000/RT)$	0
CELLA → HAA + 0.2 Glyoxal + 0.2 C ₂ H ₄ O + 0.25 HMFU + 0.2 C ₃ H ₆ O + 0.22 CO ₂ + 0.16 CO + 0.1 CH ₄ + 0.01G{H ₂ } + 0.83 H ₂ O + 0.01 HCOOH + 0.61 Char	$1 \times 10^9 \exp(-30000/RT)$	650
CELLA → LVG	$4 \times T \exp(-10000/RT)$	490
CELL → 5 H ₂ O + 6 Char	$8 \times 10^7 \exp(-31000/RT)$	-1800
HCE → 0.4 HCE1 + 0.6 HCE2	$1 \times 10^{10} \exp(-31000/RT)$	100
HCE1 → 1.025 G{H ₂ } + 0.025 H ₂ O + 1.075 CO ₂ + 0.025 HCOOH + 1.1 CO + 0.3 CH ₂ O + 0.125 C ₂ H ₅ OH + 0.25 G{CH ₃ OH} + 0.625 CH ₄ + 0.25 C ₂ H ₄ + 0.875 Char	$3 \times 10^9 \exp(-32000/RT)$	22
HCE1 → 0.4 G{H ₂ } + 0.25 H ₂ O + 0.75 CO ₂ + 0.05 HCOOH + 0.7 CO + 0.15 G{CO} + 1.3 G{COH ₂ } + 0.625G{CH ₄ } + 0.15×T exp(-8000/RT) 0.375G{C ₂ H ₄ } + 0.675 Char		-1400
HCE1 → XYLAN	$3 \times T \exp(-11000/RT)$	590
HCE2 → 0.2 H ₂ O + 0.425 CO ₂ + 0.55 G{CH ₄ } + 0.275 G{C ₂ H ₄ } + 0.1 CH ₂ O + 0.1 C ₂ H ₅ OH + 0.2 HAA + 0.025 HCOOH + 0.55 G{CO ₂ } + 0.2 CO + G{COH ₂ } + 0.325G{H ₂ } + Char	$1 \times 10^{10} \exp(-33000/RT)$	-330
LIG-C → 0.35 LIGCC + 0.1 COUMARYL + 0.08 PHENOL + 0.41 C ₂ H ₄ + H ₂ O + G{COH ₂ } + 0.495 CH ₄ + 0.32 CO + 5.735 Char	$4 \times 10^{15} \exp(-48500/RT)$	-100
LIG-H → LIGOH + C ₃ H ₆ O	$2 \times 10^{13} \exp(-37500/RT)$	130
LIG-O → LIGOH + CO ₂	$1 \times 10^9 \exp(-25500/RT)$	260
LIGCC → 0.3 COUMARYL + 0.2 PHENOL + 0.35 HAA + 0.7 H ₂ O + 0.65 G{CH ₄ } + 0.6 G{C ₂ H ₄ } + G{COH ₂ } + 0.4 G{CO} + 0.4 CO + 6.75 Char	$5 \times 10^6 \exp(-31500/RT)$	-450
LIGOH → LIG + 0.15 G{H ₂ } + 0.9 H ₂ O + 0.5 CH ₃ OH + 0.5 G{CH ₃ OH} + 0.05 CO ₂ + 0.3 CO + G{CO} + 0.05 HCOOH + 0.6 G{COH ₂ } + 0.45 G{CH ₄ } + 0.2 G{C ₂ H ₄ } + 4.15 Char	$3 \times 10^8 \exp(-30000/RT)$	70
LIGOH → 1.3 G{H ₂ } + 1.5 H ₂ O + 0.5 CO ₂ + 1.6 G{CO} + 3.9 G{COH ₂ } + 1.45G{CH ₄ } + 0.7 C ₂ H ₄ + 10.15 Char	$1 \times 10^2 \exp(-15000/RT)$	-1300
LIG → FE2MACR	$8 \times T \exp(-12000/RT)$	890
LIG → 0.95 H ₂ O + 0.2 CH ₂ O + 0.2 C ₂ H ₄ O + 0.4 CH ₃ OH + CO + 0.2 C ₃ H ₆ O + 0.6 G{CH ₄ } + 0.65 G{C ₂ H ₄ } + 0.05 HCOOH + 0.45 G{CO} + 0.5 G{COH ₂ } + 5.5 Char	$1.2 \times 10^9 \exp(-30000/RT)$	-300
LIG → G{CH ₄ } + 0.5 G{C ₂ H ₄ } + 0.4 G{H ₂ } + 0.6 H ₂ O + 0.4 CO + 0.4 CO ₂ + 0.2 G{CO} + 2 G{COH ₂ } + 6 Char	$0.25 \times T \times \exp(-8000/RT)$	-1770
G{CO ₂ } → CO ₂	$6 \times 10^5 \exp(-24000/RT)$	-860
G{CO} → CO	$5 \times 10^{11} \exp(-50000/RT)$	-1500
G{COH ₂ } → CO + H ₂	$5 \times 10^{11} \exp(-71000/RT)$	6800
G{H ₂ } → H ₂	$5 \times 10^{11} \exp(-75000/RT)$	0
G{CH ₄ } → CH ₄ G{C ₂ H ₄ } → C ₂ H ₄ G{CH ₃ OH} → CH ₃ OH	$0.5 \times 10^{13} \exp(-50000/RT)$	0

* Activation energy expressed in kcal/kmol

4. Thermal behaviour of thick particle pyrolysis

Figure 3 shows a comparison between experimental and predicted profiles of centre temperature, for the induction-furnace experiments described above. Experimental results in this figure were obtained for three pyrolysis temperatures: 723, 923 and 1023 K. The profiles show the presence of two thermal regimes during wood pyrolysis. For the three cases studied, temperature first increases until reaching an inflexion point respectively at 300, 190 and 160s. From this inflexion point, temperature strongly increases, even exceeding the steady state plateau when pyrolysis temperature is 723 K.

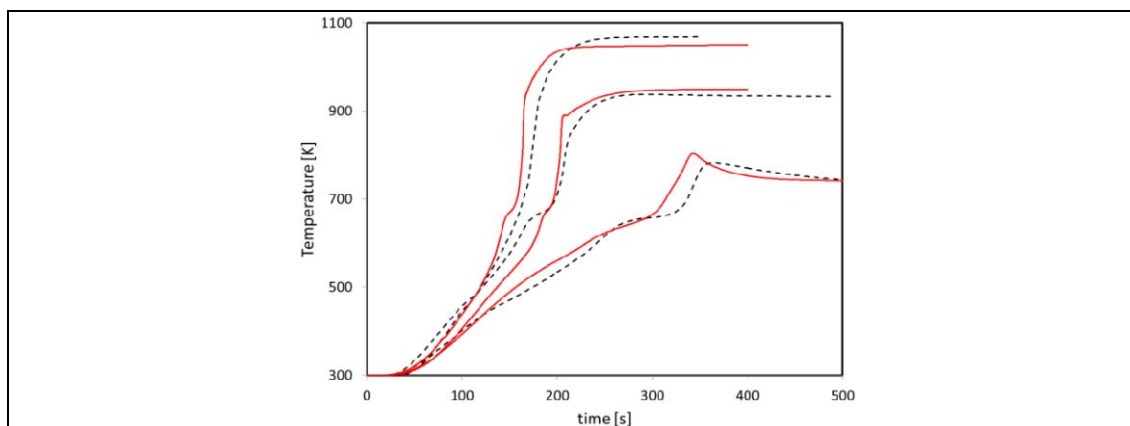


Figure 3: Centre temperature comparison between the proposed model (solid lines) and the experiments (dotted lines)

Figure 4.a shows the comparison between experiment and mechanism, for the nitrogen-heated experiments described above. In these measurements significant temperature gradients are observed inside the wood particle. There is a plateau at about 650 K and a maximum in the temperature profile. It seems also relevant to observe that wood particles are anisotropic and subject to splitting, in some experiments. This is a further complicating aspect. Figure 4.b shows a comparison between observed center temperatures for split and unsplit particles.

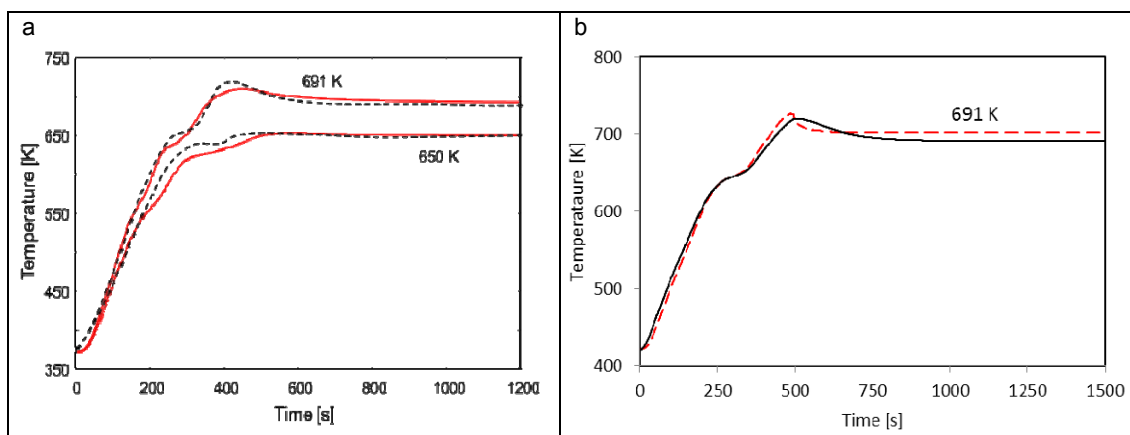


Figure 4: a: Centre temperature comparison between the proposed model (solid lines) and the experiments of (Bennadji et al. 2013) (dotted lines); $D=1.9$ cm. b: Comparison of the experimental center temperature for un-split (solid line) and split (dashed line) particles with $D=2.54$ cm.

Similarly, (Park et al. 2010) studied the pyrolysis of thick wood spheres in the temperature range 638-879 K. A comparison of experimental and predicted solid mass loss and temperature profiles for a furnace temperature of 688 K is shown in Figure 5.a. At 688 K, endothermic reactions cause a centre temperature plateau, with a large decrease of solid residue. Then, a steep temperature increase with the centre temperature peak exceeding the surface temperature is observed at low temperatures, with a negligible amount of further solid mass loss (Figure 5.b).

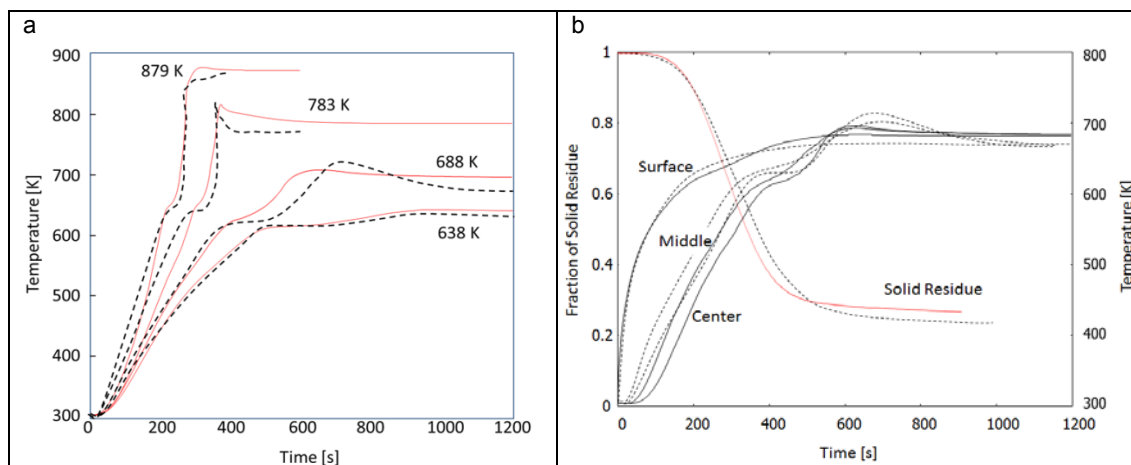


Figure 5.a: Centre temperature comparison between the proposed model (solid lines) and the experiments of (Park et al. 2010) (dotted lines). b: Solid mass fraction of wood sphere at 688 K. Comparison between the proposed model (solid lines) and the experiments of (Park et al. 2010) (dotted lines).

The general behavior of these temperature profiles is very similar in the three experimental studies considered. Mainly at low temperatures, the centre temperature shows a flat plateau at ~ 650 K followed by a maximum temperature higher than the external one. Similar results were already discussed by (Milosavljevic et al. 1996) when studying the thermochemistry of cellulose pyrolysis. They concluded, on the basis of several reliable pieces of experimental evidence, that the endothermicity of the process mainly reflects the latent heat requirement for vaporizing the tar decomposition products. In contrast, the exothermic character of char formation, which depends on the reaction conditions, is the reason for the occurrence of a maximum in centre temperature.

5. Conclusion

Pyrolysis tests are carried out in a new device for temperatures ranging between 723 K and 1073 K. Internal temperatures are measured continuously during the pyrolysis of a centimetre-scale wood sample. These experimental results with the ones of (Park et al. 2010) and (Bennadji et al. 2013) enable the validation of an extended version of the multistep kinetic model developed by (Ranzi et al. 2008).

Any feedstock is considered as a mixture of reference components: cellulose, hemicelluloses, and lignins. The kinetic model is coupled to a one-dimensional spherical, isotropic-property description of the species and temperature gradients inside the particle.

The extended model is used to simulate the three experimental data sets. The comparison is satisfactory and highlights that at low temperatures, the temperatures at the sample centre show a plateau followed by a peak. This can be explained by the release of tar components which competes with vaporization (endothermic) and cross-linking reactions with an increase of residual char (exothermic). (Bennadji et al. 2013)

References

- Bennadji, H., Smith, K., Shabangu, S., Fisher M., E. (2013) 'Low-temperature pyrolysis of woody biomass in the thermally thick regime', *Energy and Fuels*, 27, 1453-1459.
- Blondeau, J., Jeanmart, H. (2012) 'Biomass pyrolysis at high temperatures: prediction of gaseous species yields from an anisotropic particle', *Biomass and Bioenergy* 41, 107-121.
- Catoire, L., Yahyaoui, M., Osmont, A., Gokalp, I. (2008) 'Thermochemistry of Compounds Formed during Fast Pyrolysis of Lignocellulosic Biomass', *Energy & Fuels*, 22(6), 4265-4273.
- Mendes, F., Figueiredo, M. (2011) 'Problems Recorded on the Appropriateness of a Pilot Plant for Production of Second Generation Biofuels by Fast Pyrolysis', *Chemical Engineering Transactions*, 24.
- Milosavljevic, I., Oja, V., Suuberg, E. M. (1996) 'Thermal effects in cellulose pyrolysis: Relationship to char formation processes.' *Industrial & Engineering Chemistry research*, 35(3), 653-662.
- Park, W. C., Atreya, A., Baum, H. R. (2010) 'Experimental and theoretical investigation of heat and mass transfer processes during wood pyrolysis', *Combustion and Flame*, 157(3), 481-494.
- Ranzi, E., Cuoci, A., Faravelli, T., Frassaldati, A., Migliavacca, G., Pierucci, S., Sommariva, S. (2008) 'Chemical Kinetics of Biomass Pyrolysis', *Energy Fuels*, 22, 4292-4300.